

# Aberrant Expression of GABA-Related Genes in the Hippocampus of 3xTg-AD Model Mice from the Early to End Stages of Alzheimer's Disease

Hiroaki Mori, Yuta Yoshino, Jun-ichi Iga\*, Shinichiro Ochi, Yu Funahashi, Kiyohiro Yamazaki, Hiroshi Kumon, Yuki Ozaki and Shu-ichi Ueno  
*Department of Neuropsychiatry, Molecules and Function, Ehime University Graduate, School of Medicine, Shitsukawa, Toon, Ehime, Japan*

Accepted 14 April 2023  
Pre-press 18 May 2023

## Abstract.

**Background:** We explored the gene expression levels in the brain of 3xTg-AD model mice to elucidate the molecular pathological changes from the early to end stages of Alzheimer's disease (AD).

**Objective:** We re-analyzed our previously published microarray data obtained from the hippocampus of 3xTg-AD model mice at 12 and 52 weeks of age.

**Methods:** Functional annotation and network analyses of the up- and downregulated differentially expressed genes (DEGs) in mice aged 12 to 52 weeks were performed. Validation tests for gamma-aminobutyric acid (GABA)-related genes were also performed by quantitative polymerase chain reaction (qPCR).

**Results:** In total, 644 DEGs were upregulated and 624 DEGs were downregulated in the hippocampus of both the 12- and 52-week-old 3xTg-AD mice. In the functional analysis of the upregulated DEGs, 330 gene ontology biological process terms, including immune response, were found, and they interacted with each other in the network analysis. In the functional analysis of the downregulated DEGs, 90 biological process terms, including several terms related to membrane potential and synapse function, were found, and they also interacted with each other in the network analysis. In the qPCR validation test, significant downregulation was seen for *Gabrg3* at the ages of 12 ( $p=0.02$ ) and 36 ( $p=0.005$ ) weeks, *Gabbr1* at the age of 52 weeks ( $p=0.001$ ), and *Gabbr2* at the age of 36 weeks ( $p=0.02$ ).

**Conclusion:** Changes in immune response and GABAergic neurotransmission may occur in the brain of 3xTg mice from the early to end stages of AD.

Keywords: Alzheimer's disease, GABA, gene expression, microarrays, 3xTg-AD model mice

## INTRODUCTION

Alzheimer's disease (AD) is a neurodegenerative disorder with recent memory impairment as the core

symptom, but it often presents with psychiatric symptoms, such as anxiety and depression [1, 2]. There is currently no cure, and all treatments are palliative and have limited effects on the disease progression and pathogenesis. The histopathological hallmarks in the AD brain are senile plaques and neurofibrillary tangles [3, 4]. Senile plaques are extracellular accumulations of amyloid- $\beta$  beta ( $A\beta$ ) produced from the amyloid- $\beta$  protein precursor ( $A\beta$ PP) [5],

\*Correspondence to: Jun-ichi Iga, Department of Neuropsychiatry, Molecules and Function, Ehime University Graduate, School of Medicine, Shitsukawa, Toon, Ehime 791-0295, Japan. Tel.: +81 89 960 5315; Fax: +81 89 960 5317; E-mail: iga.junichi.it@ehime-u.ac.jp; ORCID: <https://orcid.org/0000-0003-4409-3096>.

which is encoded by the *APP* gene located at chromosome 21q21.3. Neurofibrillary tangles are abnormal intracellular accumulations of hyperphosphorylated protein tau, which are encoded by the microtubule-associated protein tau gene (*MAPT*) [6]. *APP* mutations are linked to familial AD and cerebral amyloid angiopathy [7]. *MAPT* mutations are associated with frontotemporal dementia with parkinsonism linked to chromosome 17 (FTDP-17), which causes abnormal tau aggregation [8]. Mutations in the presenilin 1 gene (*PSEN1*) encoding presenilin-1 at chromosome 14q24.2 enhance A $\beta$  generation, and have been reported as the most common cause of familial AD [9]. Similarly, mutations in the presenilin 2 gene (*PSEN2*) at chromosome 1q42.13 have been reported as the main cause of familial AD [9].

3xTg-AD model mice have three mutations (Swedish *APP*, *PSEN1* M146V, and *MAPT* P301L) associated with familial AD, and exhibit both the plaque and tangle pathologies [10]. At as early as 3 to 4 months of age, intracellular A $\beta$  immunoreactivity is detected in several brain regions [10]. Extracellular accumulation of A $\beta$  in the frontal cortex appears within 6 months of age and becomes more widespread by 12 months of age [11]. Abnormal aggregates of hyperphosphorylated tau in the hippocampus appear within 12 to 15 months of age [10]. Synaptic dysfunction, including long-term potentiation impairments, occurs prior to the development of senile plaques and neurofibrillary tangles [10]. Cognitive impairment is observed by 4 months of age [12]. 3xTg-AD model mice are considered one of the most promising AD model mice [13].

The amyloid cascade hypothesis, which posits that the neurodegenerative pathology of AD is caused by the accumulation of A $\beta$  plaques, has widely been accepted [14, 15]. However, many drugs designed to eliminate the extracellular accumulation of A $\beta$  have failed to improve the symptoms of AD [16–18]. Recent studies have suggested that the intracellular accumulation of soluble A $\beta$  is more neurotoxic and plays a more important role in AD pathology than the extracellular accumulation of insoluble A $\beta$  fibers [19–21]. Thus, this study was designed to evaluate the genetic changes in the brain of 3xTg mice at 12 weeks when only intracellular accumulation of soluble A $\beta$  was observed [10].

In addition, it has been suggested that aberrant gamma-aminobutyric acid (GABA) neurotransmission may be present in AD model mice and AD patients [22, 23], but the details remain unknown.

Therefore, we focused and investigated on GABA-related genes.

In this study, to elucidate the changes in gene expression over time from the early to end stages of AD, we performed 1) a microarray analysis using the hippocampus of 3xTg-AD model mice at 12 and 52 weeks of age, 2) functional annotation and network analyses of the up- and downregulated differentially expressed genes (DEGs) in mice aged 12 to 52 weeks, and 3) reverse transcription-quantitative polymerase chain reaction (qPCR) validation tests for GABA-related genes.

## MATERIALS AND METHODS

### *Animal models*

The male 3xTg-AD mice were purchased from Jackson Laboratory (MMRRC #34830; B6129SF1/J, JAX #101043). As the sham group, male B6129SF2 wild-type (WT) mice were purchased and age-matched with the 3xTg mice ( $n=8$  each at 12, 36, and 52 weeks of age). In the 3xTg mice, the ages of 12, 36, and 52 weeks were chosen to represent the early, middle, and late stages of AD [24, 25]. The sample size ( $n=8$  each) was the minimum number required for the experiment, and the number permitted by the Ethics Committee of Ehime University. The mice were housed in a pathogen-free environment with a 12-h light/12-h dark cycle at room temperature (22°C) with 50% humidity and climate control. The mice were given unlimited access to water and standard food (Oriental Yeast Co., Ltd.). At 12, 36, or 52 weeks of age, the mice were anesthetized and killed by decapitation. Each hippocampus was immediately excised and frozen at  $-80^{\circ}\text{C}$  for RNA isolation. All of the animal experiments were approved by the Animal Experiment Committee of Ehime University (#28-25).

### *Microarray analysis*

Microarray data from our previous study [26] using the hippocampus of 12- and 52-week-old mice were re-analyzed. The microarray data were deposited into the GEO database (accession number GSE144459). Total RNA was isolated from the frozen hippocampus using the RNeasy Mini Kit (QIAGEN, #74104). A NanoDrop1000 device (Thermo Fisher Scientific) was used to measure the concentrations of RNA. An Agilent 2100 Bioanalyzer (Agilent) was

used to measure the RNA integrity number (RIN). All of the samples used for the microarray analysis satisfied the following criteria:  $A260/A280 \geq 1.8$ ,  $A260/A230 \geq 2.0$ , and  $RIN \geq 7.0$ . The RIN of each sample is shown in Supplementary Table 1.

#### *Analysis of microarray data*

Probes showing no signal or an extremely low signal in all groups of mice were omitted as they indicated unreliable signals or low expression. Probe sets registered as mRNA sequences in the National Center for Biotechnology Information (NCBI) Reference Sequence Database (<https://www.ncbi.nlm.nih.gov/refseq/>) were analyzed. Probes that have been detected as transcript variants registered in the NCBI Reference Sequence Database were removed. When multiple probes were registered for one gene symbol, only the probe showing the highest expression level was selected. The average expression levels of the WT and 3xTg mice were compared by Student's *t*-test using R software (R version 4.0.2) [27]. Statistical significance for DEGs was defined as a  $p$ -value  $< 0.05$  and  $q$ -value  $< 0.05$ . The Ggplot2 R package was used to generate volcano plots. The Heatmap2 R package was used to generate heatmaps based on the DEGs that showed a significant change.

#### *Pathway and process enrichment analyses*

Gene ontology analysis of the biological processes (BPs) based on the up- or downregulated DEGs in the 12- and 52-week-old groups was performed using Metascape (<https://metascape.org/>) [28]. Using the cumulative hypergeometric distribution,  $p$ -values were computed. Terms with a  $p$ -value  $< 0.01$  ( $-\text{Log}_{10} p$ -value  $> 2$ ) and a minimum count of three genes were collected and grouped into clusters based on their similarities. For hierarchical clustering of the enriched terms, kappa scores were utilized as the similarity measure, and sub-trees with a similarity of  $> 0.3$  were regarded as a cluster. The terms with the lowest  $p$ -values from each cluster were chosen as cluster labels. To visualize the links between terms, a graphical network of enriched terms was created by Metascape [28] and Cytoscape (<https://www.cytoscape.org/>) [29]. Each node representing an enriched term was colored according to the  $p$ -value. Terms with a similarity  $> 0.3$  were connected by edges. Only term labels with the lowest  $p$ -values from each cluster are shown, and only the

network plots with more than three enriched terms are displayed.

#### *qPCR*

To measure the expression levels of mRNA, qPCR was performed using the StepOnePlus Real-Time PCR System (Applied Biosystems). The predesigned Prime-Time qPCR Assays (Integrated DNA Technologies, Inc.) were used as probes to evaluate the expression levels of each mRNAs and shown in Supplementary Table 2. Gapdh was used as the reference gene. The Prime-Time Gene Expression Master Mix (Integrated DNA Technologies, Inc.) was used in a final volume of 10  $\mu\text{L}$ . To eliminate errors between plates, the same calibrator sample was included on each plate. mRNA expression levels were measured in duplicate. The  $\Delta\Delta\text{Ct}$  method [30] was used to calculate the relative expression values.

#### *Statistical analysis*

SPSS 22.0 software (IBM Japan) was used for the statistical analysis of the qPCR results. The evaluation of data with a normal distribution was conducted using the Shapiro–Wilk test. Student's *t*-test or the Mann-Whitney U test were used to compare the average mRNA expression levels between the WT and 3xTg mice. A 95% threshold of statistical significance ( $p = 0.05$ ) was used.

## **RESULTS**

#### *Data of the microarray analysis*

A total of 10,599 genes met the criteria. In the 12-week-old group, 923 upregulated (Supplementary Table 3) and 1,332 downregulated (Supplementary Table 4) DEGs were detected in the 3xTg mice when compared to the WT mice ( $p < 0.05$  and  $q < 0.05$ ). The heatmaps of the DEGs in the 12-week-old group are shown in Fig. 1A. In the 52-week-old group, 1,928 upregulated (Supplementary Table 5) and 1,728 downregulated (Supplementary Table 6) DEGs were detected in the 3xTg mice when compared to the WT mice ( $p < 0.05$  and  $q < 0.05$ ). The heatmaps of the DEGs in the 52-week-old group are shown in Fig. 1B. The DEGs with a high fold-change are shown in Table 1. The DEGs that overlapped in each group are shown in the Venn diagram in Fig. 1C. In total, 644 DEGs were upregulated and 624 DEGs were downregulated in both the 12- and 52-week-old groups.

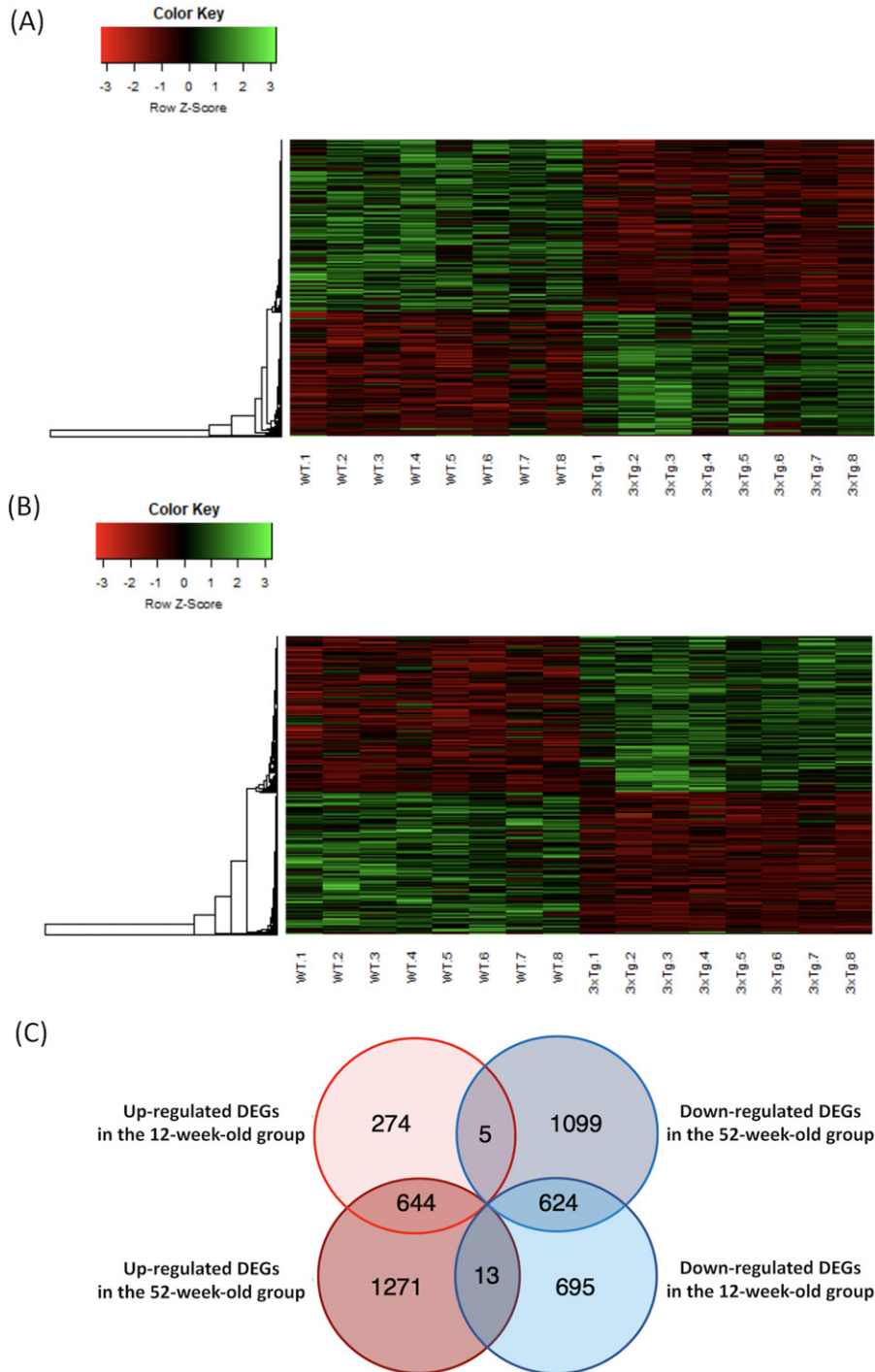


Fig. 1. Heatmap of the microarray data, and Venn diagram of the overlapping DEGs in each group. A) The microarray data of DEGs in the 12-week-old group were plotted as a heatmap. High-expression DEGs are shown in red, and low-expression DEGs are shown in green. B) The microarray data of DEGs in the 52-week-old group were plotted as a heatmap. C) The number of DEGs that overlapped in each group are shown in the Venn diagram. DEGs, differentially expressed genes; WT, wild-type mice; 3xTg, 3xTg-AD model mice.

Table 1  
Top five DEGs with the highest fold-change among the significantly up- and downregulated genes in the 12- and 52-week-old groups

Gene symbol	Average of the normalized data in WT mice	Average of the normalized data in 3xTg mice	Log <sub>2</sub> fold-change	p	q
Top five upregulated DEGs with the highest fold-change in the 12-week-old group					
Cxcl13	0.050408952	2.820469316	5.806111471	0.003445821	0.024496812
Oasl2	0.584399695	9.36622486	4.002440344	0.009011224	0.044882502
Ccl5	0.541773611	8.160814155	3.912951058	0.005021155	0.030657232
Ifit1	0.53996433	6.762051803	3.646525057	0.003314123	0.024003804
Cxcl10	0.401585376	4.578947735	3.511237461	0.00422173	0.027861664
Top five downregulated DEGs with the highest fold-change in the 12-week-old group					
Ccl21a	25.37164157	0.627859098	-5.336632226	9.66527E-06	0.000806631
Zfp874a	43.45221774	1.276459608	-5.089210021	1.02272E-05	0.000829015
Rbbp9	27.01882468	0.848187133	-4.993438511	0.001395976	0.014530777
Ttll2	3.555112353	0.334358437	-3.410427728	1.44854E-05	0.001030408
Fam205a2	8.844129732	0.879447808	-3.330050321	0.000149049	0.004109068
Top five upregulated DEGs with the highest fold-change in the 52-week-old group					
Kcnj13	0.385411	4.692683	3.605942	0.017019	0.049461
Cxcl13	0.90027	10.00182	3.473762	7.94E-05	0.001068
Apol11b	0.56543	5.447487	3.268169	1.45E-05	0.000355
Ttr	0.290173	2.773204	3.256569	0.008109	0.0285
Ccl5	0.821118	7.783114	3.244685	0.002888	0.013298
Top five downregulated DEGs with the highest fold-change in the 52-week-old group					
Rbbp9	29.2128	0.294613	-6.63163	0.00014	0.001569
Fam205a2	5.268748	0.287721	-4.19472	0.00635	0.023892
Ttll2	5.200771	0.501302	-3.37497	0.000237	0.00228
Gm20878	2.261651	0.461658	-2.29248	5.06E-12	1.07E-08
Gm1987	3.487344	0.729345	-2.25746	0.011973	0.037961

DEGs, differentially expressed genes; WT, wild-type; 3xTg, 3xTg-AD model.

Lists of the genes that overlapped in each group are shown in Supplementary Table 7A-D.

#### Functional annotation and network analysis

All of the 644 upregulated DEGs in both the 12- and 52-week-old groups were subjected to functional annotation analysis. There were 330 BP terms that reached a significant level (Supplementary Table 8). Hierarchical clustering of the enriched terms was performed, and the terms with the lowest  $p$ -values from each cluster were chosen as cluster labels. The top 20 cluster labels are shown in Fig. 2A. The network of the 330 significant BP terms is shown in Fig. 2B. Several terms related to immune response (response to interferon-gamma, defense response to virus, etc.) were found, and they interacted with each other. Response to interferon-gamma was the most significant term ( $p < 0.001$ ;  $-\log_{10} p$  value = 11.5).

All 624 downregulated DEGs in both the 12- and 52-week-old groups were also subjected to functional annotation analysis. Among the terms for the 624 downregulated DEGs, 90 BP terms were found as significant terms (Supplementary Table 9). Hierarchical

clustering of the enriched terms was performed, and the terms with the lowest  $p$ -values from each cluster were chosen as cluster labels. The top 20 cluster labels are shown in Fig. 3A. The network of the 90 significant BP terms is shown in Fig. 3B. Some terms related to membrane potential were found, and they interacted with each other in the network analysis. In addition, some terms related to synapse function (long-term synaptic depression, gamma-aminobutyric acid signaling pathway, etc.) were found, and they interacted with each other. Regulation of sinoatrial node cell action potential was the most significant term ( $p < 0.001$ ,  $-\log_{10} p$  value = 4.8).

#### qPCR validation for microarray data

The expression levels of mRNA in the hippocampus were compared between the WT and 3xTg mice ( $n = 8$  each at 12, 36, and 52 weeks). For functional annotation of the 624 downregulated genes, we focused on the GABA signaling pathway, because aberrant GABA neurotransmission was previously reported in AD model mice and AD patients [22, 23]. Four genes associated with the GABA signaling

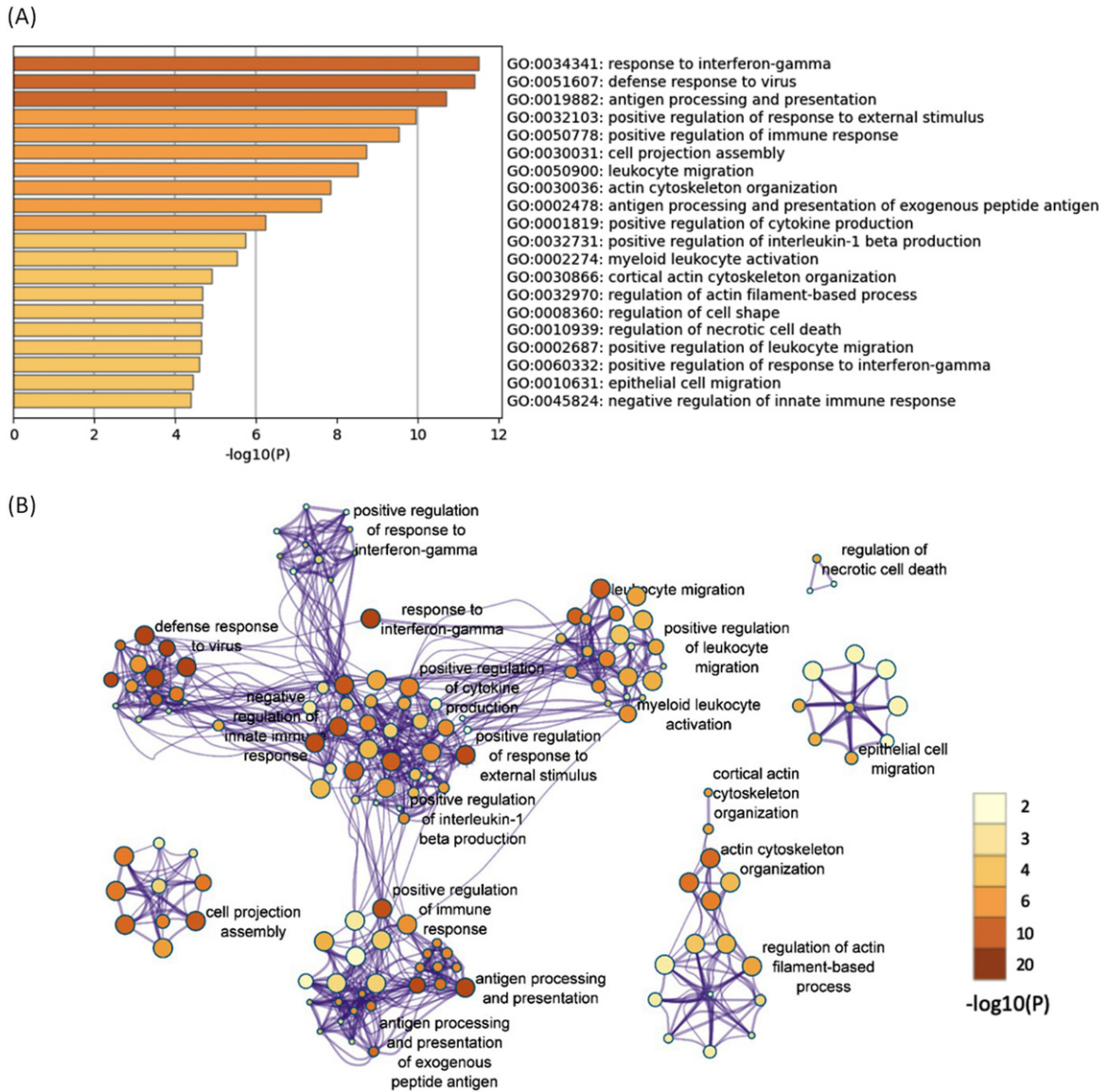


Fig. 2. The enriched BP terms of the upregulated DEGs in both the 12- and 52-week-old groups. A) Bar graph of the top 20 enriched BP terms of the upregulated DEGs in both the 12- and 52-week-old groups colored according to the  $p$ -value. B) Network plots of the enriched BP terms. Each node represents an enriched term that is colored according to the  $p$ -value. Terms with a similarity  $> 0.3$  are connected by edges. Hierarchical clustering of the enriched terms was performed, and only the annotations of the terms with the most significant  $p$ -values from each cluster are shown. Only the network plots with more than three enriched terms are displayed. DEGs, differentially expressed genes; BP, biological process.

pathway (Gabrg3, Gabrr2, Gabbr1, and Gabra1) were chosen from among the significantly downregulated DEGs in all groups. Significant changes were found in Gabrg3 in the 12- ( $p=0.02$ ) and 36- ( $p=0.005$ ) week-old groups, Gabbr1 in the 52-week-old group ( $p=0.001$ ), and Gabrr2 in the 36-week-old group ( $p=0.02$ ) (Table 2, Fig. 4). In Gabrr1 in the 52-week-old group, there was a significant difference between

the two groups even when the potential outlier was removed ( $p=0.001$ ). These qPCR validation results were consistent with the microarray data. On the other hand, no significant changes were observed for Gabrg3 in the 52-week-old group ( $p=0.08$ ), Gabbr1 in the 12- ( $p=0.12$ ) and 36- ( $p=0.09$ ) week-old groups, Gabrr2 in the 12- ( $p=0.73$ ) and 52- ( $p=0.53$ ) week-old groups, and Gabra1 in the 12- ( $p=0.87$ ),

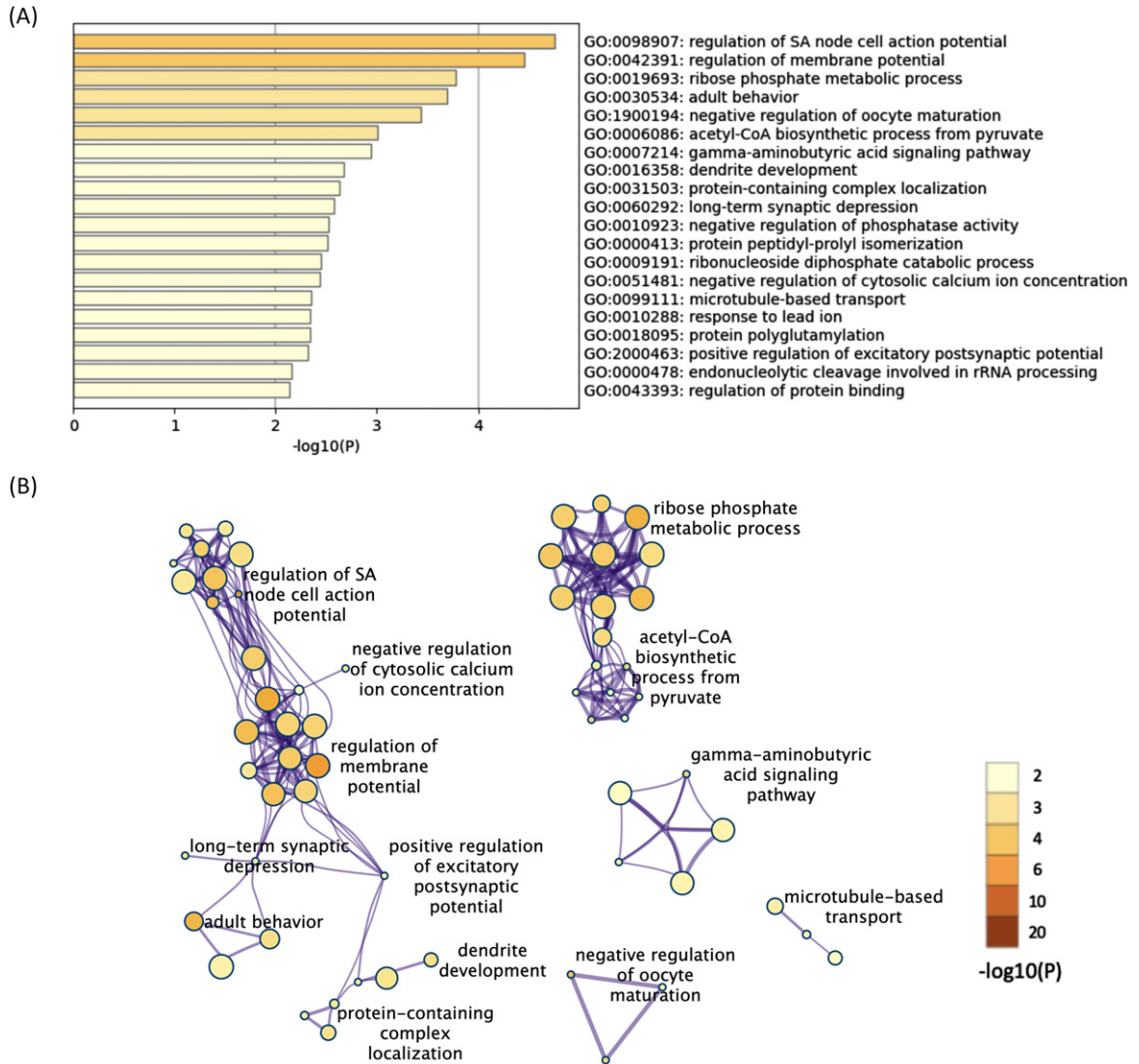


Fig. 3. The enriched BP terms of the downregulated DEGs in both the 12- and 52-week-old groups. A) Bar graph of the top 20 enriched BP terms of the downregulated DEGs in both the 12- and 52-week-old groups colored according to the  $p$ -value. B) Network plots of the enriched BP terms in both the 12- and 52-week-old groups. Each node represents an enriched term that is colored according to the  $p$ -value. Terms with a similarity  $> 0.3$  are connected by edges. Hierarchical clustering of the enriched terms was performed, and only term labels with the most significant  $p$ -values from each cluster are shown. Only the network plots with more than three enriched terms are displayed. DEGs, differentially expressed genes; BP, biological process.

36- ( $p=0.11$ ), and 52- ( $p=0.31$ ) week-old groups (Table 2, Fig. 4).

## DISCUSSION

This is the first study to investigate the changes in the gene expression levels from the early stage (12 weeks of age) to the end stage (52 weeks of age) of AD in 3xTg-AD model mice. We previ-

ously used the same microarray data to explore blood biomarkers of AD [26]. The methods used in the present study differed from those of the previous study in that transcription variants were removed and the statistical significance level was tightened, allowing us to detect genes with higher certainty. We found 644 upregulated and 624 downregulated genes that showed changes in the expression levels over time. We then focused on GABA-related genes from the

Table 2  
The expression levels of GABA-related genes in each group

	WT mice	3xTg mice	<i>p</i>
Gabra1 expression in 12-week-old	1.00 ± 0.07	0.99 ± 0.06	0.87
Gabra1 expression in 36-week-old	1.11 ± 0.06	1.05 ± 0.06	0.11
Gabra1 expression in 52-week-old	0.87 ± 0.08	0.84 ± 0.02	0.31
Gabbr2 expression in 12-week-old	1.00 ± 0.25	0.95 ± 0.25	0.73
Gabbr2 expression in 36-week-old	1.69 ± 0.49	1.13 ± 0.17	0.02
Gabbr2 expression in 52-week-old	1.27 ± 0.50	1.44 ± 0.45	0.53
Gabrg3 expression in 12-week-old	1.00 ± 0.08	0.88 ± 0.09	0.02
Gabrg3 expression in 36-week-old	1.12 ± 0.14	0.92 ± 0.09	0.005
Gabrg3 expression in 52-week-old	0.78 ± 0.10	0.70 ± 0.05	0.08
Gabbr1 expression in 12-week-old	1.00 ± 0.04	0.95 ± 0.04	0.12
Gabbr1 expression in 36-week-old	0.99 ± 0.04	0.97 ± 0.03	0.09
Gabbr1 expression in 52-week-old	1.03 ± 0.17	0.89 ± 0.04	0.001

Values are means ± standard deviation. The expression levels of GABA-related genes in each group are shown divided by the average expression level in WT mice at 12-week-old. WT, wild-type; 3xTg, 3xTg-AD model.

functional annotation results of the 624 downregulated genes and found from the qPCR validation tests that the expression levels of several GABA-related genes were significantly decreased.

In the functional and network analyses of the upregulated DEGs, several terms related to immune response were found. Several studies have previously reported neuroinflammation in the AD brain [31, 32]. Microglia are involved in neuroinflammation in the AD brain by releasing inflammatory mediators [33]. As soon as A $\beta$  plaques form in the brain, microglia establish intimate contact with the plaques and become reactive [34, 35]. A vicious cycle of inflammation is thus formed between A $\beta$  accumulation, activated microglia, and microglial inflammatory mediators, further enhancing A $\beta$  deposition and neuroinflammation [33]. Previous studies have suggested that the use of non-steroidal anti-inflammatory drugs (NSAIDs) may protect against AD [36]. The results of the present study suggest that abnormal neuroimmune responses may occur even at the early stage of AD.

The downregulated DEGs were found to be related to membrane potential and synapse function, including the GABA signaling pathway. GABAergic inhibitory neurotransmission plays a central role in regulating, synchronizing, and preventing excessive neuronal signaling in the hippocampus [37, 38], which is important for episodic memory [39–41]. In both AD patients and mice, abnormal A $\beta$  production and aggregation decrease the number and activity of GABAergic inhibitory interneurons [42–45]. In several postmortem studies, reduced GABA levels have been found in the brain of AD patients [46–49]. Several studies have reported a decreased concentration

or expression level of GABAA receptor subunits in the hippocampus of AD patients [50–52]. Furthermore, hippocampal neural hyperactivity due to the loss of GABAergic interneurons has been confirmed in AD model mice and AD patients [53–56], and may predict atrophy and reduced episodic memory in individuals at risk for AD [57]. In addition, some studies have reported that seizures in AD patients may be a product of neural hyperactivity due to GABAergic signaling dysfunction [58]. Furthermore, levetiracetam, an antiepileptic drug that enhances GABA function and inhibits hippocampal hyperexcitability [59], has been reported to improve cognitive function in AD-model mice [60, 61], AD patients [62], and mild cognitive impairment patients [63, 64]. Based on several lines of evidence, GABAergic signaling dysfunction might play an important role in the pathogenesis of AD. In the present study, the downregulated expression of Gabrg3, which encodes the GABAA receptor  $\gamma$  subunit, was confirmed in 12-week-old 3xTg mice. The early abnormalities in the GABA neurotransmitters observed in this study may be involved in the progression of the AD pathology. In qPCR results at 52 weeks, the expression levels of most GABA-related genes did not differ significantly between the 3xTg model mice and the WT mice. This suggests that the expression of GABA-related genes may be associated with the effects of aging even in WT mice.

In the brain of 3xTg mice at 12 weeks of age, only intracellular accumulation of soluble A $\beta$  is detected as a major histopathological change [10]. Our present study results indicated that irreversible changes may occur in the brain of 3xTg mice at the early stage of AD when only intracellular accumulation of soluble

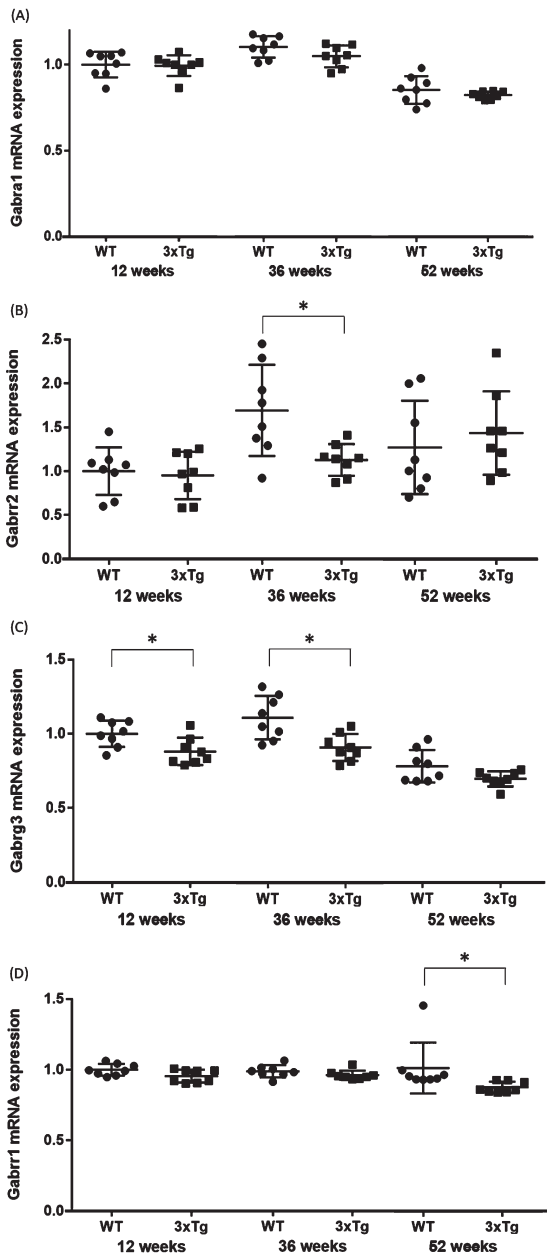


Fig. 4. Validation qPCR of the four genes associated with the GABA signaling pathway. Comparison of the (A) *Gabra1*, (B) *Gabrr2*, (C) *Gabrg3*, and (D) *Gabrr1* mRNA expression levels between WT and 3xTg mice. The y axis represents the relative expression level (/WT mice at 12-week-old) from the qPCR results. Student's *t*-test or the Mann-Whitney U test were used to compare the average mRNA expression levels between the WT and 3xTg mice. Statistical significance was defined at  $p=0.05$ . The horizontal bars represent the means  $\pm$  standard error. \* $p < 0.05$ . WT, wild-type mice; 3xTg, 3xTg-AD model mice.

A $\beta$  is observed. This suggests the need for therapeutics targeting soluble A $\beta$  at the early stage of AD. Currently, various antibody drugs against A $\beta$  are being developed. Aducanumab, which targets insoluble A $\beta$  [65], has failed in clinical trials [15]. In contrast, clinical trials of lecanemab targeting soluble A $\beta$  [65] have achieved success [66]. The results of our present study support the validity of lecanemab.

The present study has several limitations. First, the sample size was small in the microarray analysis, and a type II error may thus be present. Second, there was no replication cohort of 3xTg mice, because no samples remained. Forth, we have no neuropathological data in this study. Therefore, the age at which amyloid and tau pathologies first appear is predicted from preceding studies. Finally, the expression level of each gene was evaluated only from the mRNA expression; the protein levels should be analyzed in future studies.

### Conclusions

Our results indicate that changes in the expression levels of genes related to immune responses and GABAergic neurotransmission may occur in the brain of 3xTg mice from the early stage of AD. This suggests the need for therapeutic intervention as early as possible in AD.

### ACKNOWLEDGMENTS

We would like to thank Ms. Chiemi Onishi for technical assistance.

### FUNDING

This study was supported by a Health and Labour Science Research Grant from the Japanese Ministry of Health, Labour and Welfare, and a Grant-in-Aid for Scientific Research from the Japanese Ministry of Education, Culture, Sports, Science and Technology (JSPS KAKENHI Grant Numbers 20K07971, 22K07597, 22K07562, 22K15765, and 22K15752). This study was supported by the Division of Laboratory Animal Research and the Division of Analytical Bio-Medicine at the Advanced Research Support Center (ADRES), Ehime University.

### CONFLICT OF INTEREST

The authors declare that they have no conflict of interest. Jun-ichi Iga is an Editorial Board Member of

this journal, but was not involved in the peer-review process, nor had access to any information regarding its peer-review.

## DATA AVAILABILITY

All microarray data have been deposited into the GEO database (accession number GSE144459).

## SUPPLEMENTARY MATERIAL

The supplementary material is available in the electronic version of this article: <https://dx.doi.org/10.3233/JAD-230078>.

## REFERENCES

- [1] Kawakami I, Iga JI, Takahashi S, Lin YT, Fujishiro H (2022) Towards an understanding of the pathological basis of senile depression and incident dementia: Implications for treatment. *Psychiatry Clin Neurosci* **76**, 620-632.
- [2] Ochi S, Mori T, Iga JI, Ueno SI (2022) Prevalence of comorbid dementia in late-life depression and bipolar disorder: A retrospective inpatient study. *J Alzheimers Dis Rep* **6**, 589-598.
- [3] Ittner LM, Gotz J (2011) Amyloid-beta and tau—a toxic pas de deux in Alzheimer’s disease. *Nat Rev Neurosci* **12**, 65-72.
- [4] Rajah Kumaran K, Yunusa S, Perimal E, Wahab H, Muller CP, Hassan Z (2023) Insights into the pathophysiology of Alzheimer’s disease and potential therapeutic targets: A current perspective. *J Alzheimers Dis* **91**, 507-530.
- [5] Cras P, Kawai M, Lowery D, Gonzalez-DeWhitt P, Greenberg B, Perry G (1991) Senile plaque neurites in Alzheimer disease accumulate amyloid precursor protein. *Proc Natl Acad Sci U S A* **88**, 7552-7556.
- [6] Goedert M, Wischik CM, Crowther RA, Walker JE, Klug A (1988) Cloning and sequencing of the cDNA encoding a core protein of the paired helical filament of Alzheimer disease: Identification as the microtubule-associated protein tau. *Proc Natl Acad Sci U S A* **85**, 4051-4055.
- [7] Grangeon L, Cassinari K, Rousseau S, Croisile B, Formaglio M, Moreaud O, Boutonnat J, Le Meur N, Mine M, Coste T, Pipiras E, Tournier-Lasserre E, Rovelet-Lecrux A, Campion D, Wallon D, Nicolas G (2021) Early-onset cerebral amyloid angiopathy and Alzheimer disease related to an APP locus triplication. *Neurol Genet* **7**, e609.
- [8] Goedert M, Spillantini MG (2000) Tau mutations in frontotemporal dementia FTDP-17 and their relevance for Alzheimer’s disease. *Biochim Biophys Acta* **1502**, 110-121.
- [9] Ryan NS, Rossor MN (2010) Correlating familial Alzheimer’s disease gene mutations with clinical phenotype. *Biomark Med* **4**, 99-112.
- [10] Oddo S, Caccamo A, Shepherd JD, Murphy MP, Golde TE, Kaye R, Metherate R, Mattson MP, Akbari Y, LaFerla FM (2003) Triple-transgenic model of Alzheimer’s disease with plaques and tangles: Intracellular Abeta and synaptic dysfunction. *Neuron* **39**, 409-421.
- [11] Belfiore R, Rodin A, Ferreira E, Velazquez R, Branca C, Caccamo A, Oddo S (2019) Temporal and regional progression of Alzheimer’s disease-like pathology in 3xTg-AD mice. *Aging Cell* **18**, e12873.
- [12] Billings LM, Oddo S, Green KN, McLaugh JL, LaFerla FM (2005) Intraneuronal Abeta causes the onset of early Alzheimer’s disease-related cognitive deficits in transgenic mice. *Neuron* **45**, 675-688.
- [13] Javonillo DI, Tran KM, Phan J, Hingco E, Kramar EA, da Cunha C, Forner S, Kawachi S, Milinkeviciute G, Gomez-Arboledas A, Neumann J, Banh CE, Huynh M, Matheos DP, Rezaie N, Alcantara JA, Mortazavi A, Wood MA, Tenner AJ, MacGregor GR, Green KN, LaFerla FM (2021) Systematic phenotyping and characterization of the 3xTg-AD mouse model of Alzheimer’s disease. *Front Neurosci* **15**, 785276.
- [14] Barage SH, Sonawane KD (2015) Amyloid cascade hypothesis: Pathogenesis and therapeutic strategies in Alzheimer’s disease. *Neuropeptides* **52**, 1-18.
- [15] Hardy JA, Higgins GA (1992) Alzheimer’s disease: The amyloid cascade hypothesis. *Science* **256**, 184-185.
- [16] Doggrell SA (2019) Lessons that can be learnt from the failure of verubecestat in Alzheimer’s disease. *Expert Opin Pharmacother* **20**, 2095-2099.
- [17] Knopman DS, Jones DT, Greicius MD (2021) Failure to demonstrate efficacy of aducanumab: An analysis of the EMERGE and ENGAGE trials as reported by Biogen, December 2019. *Alzheimers Dement* **17**, 696-701.
- [18] Salloway S, Sperling R, Fox NC, Blennow K, Klunk W, Raskind M, Sabbagh M, Honig LS, Porsteinsson AP, Ferris S, Reichert M, Ketter N, Nejadnik B, Guenzler V, Miloslavsky M, Wang D, Lu Y, Lull J, Tudor IC, Liu E, Grundman M, Yuen E, Black R, Brashear HR, Bapineuzumab 301 and 302 Clinical Trial Investigators (2014) Two phase 3 trials of bapineuzumab in mild-to-moderate Alzheimer’s disease. *N Engl J Med* **370**, 322-333.
- [19] Ferreira ST, Lourenco MV, Oliveira MM, De Felice FG (2015) Soluble amyloid-beta oligomers as synaptotoxins leading to cognitive impairment in Alzheimer’s disease. *Front Cell Neurosci* **9**, 191.
- [20] Ricciarelli R, Fedele E (2017) The amyloid cascade hypothesis in Alzheimer’s disease: It’s time to change our mind. *Curr Neuropharmacol* **15**, 926-935.
- [21] Busquets O, Parcerisas A, Verdague E, Etcheto M, Camins A, Beas-Zarate C, Castro-Torres RD, Auladell C (2021) c-Jun N-terminal kinases in Alzheimer’s disease: A possible target for the modulation of the earliest alterations. *J Alzheimers Dis* **82**(s1), S127-S139.
- [22] Shetty AK, Bates A (2016) Potential of GABA-ergic cell therapy for schizophrenia, neuropathic pain, and Alzheimer’s and Parkinson’s diseases. *Brain Res* **1638**(Pt A), 74-87.
- [23] Xu Y, Zhao M, Han Y, Zhang H (2020) GABAergic inhibitory interneuron deficits in Alzheimer’s disease: Implications for treatment. *Front Neurosci* **14**, 660.
- [24] Gimenez-Llort L, Mate I, Manassra R, Vida C, De la Fuente M (2012) Peripheral immune system and neuroimmune communication impairment in a mouse model of Alzheimer’s disease. *Ann N Y Acad Sci* **1262**, 74-84.
- [25] Rae EA, Brown RE (2015) The problem of genotype and sex differences in life expectancy in transgenic AD mice. *Neurosci Biobehav Rev* **57**, 238-251.
- [26] Ochi S, Iga JI, Funahashi Y, Yoshino Y, Yamazaki K, Kumon H, Mori H, Ozaki Y, Mori T, Ueno SI (2020) Identifying blood transcriptome biomarkers of Alzheimer’s disease using transgenic mice. *Mol Neurobiol* **57**, 4941-4951.

- [27] Team RDC (2005) A language and environment for statistical computing. *R Foundation for Statistical Computing*.
- [28] Zhou Y, Zhou B, Pache L, Chang M, Khodabakhshi AH, Tanaseichuk O, Benner C, Chanda SK (2019) Metascape provides a biologist-oriented resource for the analysis of systems-level datasets. *Nat Commun* **10**, 1523.
- [29] Shannon P, Markiel A, Ozier O, Baliga NS, Wang JT, Ramage D, Amin N, Schwikowski B, Ideker T (2003) Cytoscape: A software environment for integrated models of biomolecular interaction networks. *Genome Res* **13**, 2498-2504.
- [30] Livak KJ, Schmittgen TD (2001) Analysis of relative gene expression data using real-time quantitative PCR and the 2(-Delta Delta C(T)) Method. *Methods* **25**, 402-408.
- [31] Calsolaro V, Edison P (2016) Neuroinflammation in Alzheimer's disease: Current evidence and future directions. *Alzheimers Dement* **12**, 719-732.
- [32] Hampel H, Caraci F, Cuello AC, Caruso G, Nistico R, Corbo M, Baldacci F, Toschi N, Garaci F, Chiesa PA, Verdooner SR, Akman-Anderson L, Hernandez F, Avila J, Emanuele E, Valenzuela PL, Lucia A, Watling M, Imbimbo BP, Vergallo A, Lista S (2020) A path toward precision medicine for neuroinflammatory mechanisms in Alzheimer's disease. *Front Immunol* **11**, 456.
- [33] Cai Z, Hussain MD, Yan LJ (2014) Microglia, neuroinflammation, and beta-amyloid protein in Alzheimer's disease. *Int J Neurosci* **124**, 307-321.
- [34] Meyer-Luehmann M, Spires-Jones TL, Prada C, Garcia-Alloza M, de Calignon A, Rozkalne A, Koenigsnecht-Talboo J, Holtzman DM, Bacskai BJ, Hyman BT (2008) Rapid appearance and local toxicity of amyloid-beta plaques in a mouse model of Alzheimer's disease. *Nature* **451**, 720-724.
- [35] Prinz M, Jung S, Priller J (2019) microglia biology: One century of evolving concepts. *Cell* **179**, 292-311.
- [36] Wang J, Tan L, Wang HF, Tan CC, Meng XF, Wang C, Tang SW, Yu JT (2015) Anti-inflammatory drugs and risk of Alzheimer's disease: An updated systematic review and meta-analysis. *J Alzheimers Dis* **44**, 385-396.
- [37] Faingold CL, Gehlbach G, Caspary DM (1989) On the role of GABA as an inhibitory neurotransmitter in inferior colliculus neurons: Iontophoretic studies. *Brain Res* **500**, 302-312.
- [38] McCormick DA (1989) GABA as an inhibitory neurotransmitter in human cerebral cortex. *J Neurophysiol* **62**, 1018-1027.
- [39] Nyberg L, McIntosh AR, Houle S, Nilsson LG, Tulving E (1996) Activation of medial temporal structures during episodic memory retrieval. *Nature* **380**, 715-717.
- [40] Schacter DL, Alpert NM, Savage CR, Rauch SL, Albert MS (1996) Conscious recollection and the human hippocampal formation: Evidence from positron emission tomography. *Proc Natl Acad Sci U S A* **93**, 321-325.
- [41] Tulving E, Markowitsch HJ (1998) Episodic and declarative memory: Role of the hippocampus. *Hippocampus* **8**, 198-204.
- [42] Frere S, Slutsky I (2018) Alzheimer's disease: From firing instability to homeostasis network collapse. *Neuron* **97**, 32-58.
- [43] Palop JJ, Mucke L (2016) Network abnormalities and interneuron dysfunction in Alzheimer disease. *Nat Rev Neurosci* **17**, 777-792.
- [44] Verret L, Mann EO, Hang GB, Barth AM, Cobos I, Ho K, Devidze N, Masliah E, Kreitzer AC, Mody I, Mucke L, Palop JJ (2012) Inhibitory interneuron deficit links altered network activity and cognitive dysfunction in Alzheimer model. *Cell* **149**, 708-721.
- [45] Walsh C, Drinkenburg WH, Ahnaou A (2017) Neurophysiological assessment of neural network plasticity and connectivity: Progress towards early functional biomarkers for disease interception therapies in Alzheimer's disease. *Neurosci Biobehav Rev* **73**, 340-358.
- [46] Ellison DW, Beal MF, Mazurek MF, Bird ED, Martin JB (1986) A postmortem study of amino acid neurotransmitters in Alzheimer's disease. *Ann Neurol* **20**, 616-621.
- [47] Lowe SL, Francis PT, Procter AW, Palmer AM, Davison AN, Bowen DM (1988) Gamma-aminobutyric acid concentration in brain tissue at two stages of Alzheimer's disease. *Brain* **111**(Pt 4), 785-799.
- [48] Perry TL, Yong VW, Bergeron C, Hansen S, Jones K (1987) Amino acids, glutathione, and glutathione transferase activity in the brains of patients with Alzheimer's disease. *Ann Neurol* **21**, 331-336.
- [49] Rossor MN, Garrett NJ, Johnson AL, Mountjoy CQ, Roth M, Iversen LL (1982) A post-mortem study of the cholinergic and GABA systems in senile dementia. *Brain* **105**, 313-330.
- [50] Mizukami K, Ikonovic MD, Grayson DR, Sheffield R, Armstrong DM (1998) Immunohistochemical study of GABAA receptor alpha1 subunit in the hippocampal formation of aged brains with Alzheimer-related neuropathologic changes. *Brain Res* **799**, 148-155.
- [51] Rissman RA, Bennett DA, Armstrong DM (2004) Subregional analysis of GABA(A) receptor subunit mRNAs in the hippocampus of older persons with and without cognitive impairment. *J Chem Neuroanat* **28**, 17-25.
- [52] Rissman RA, Mishizen-Eberz AJ, Carter TL, Wolfe BB, De Blas AL, Miralles CP, Ikonovic MD, Armstrong DM (2003) Biochemical analysis of GABA(A) receptor subunits alpha 1, alpha 5, beta 1, beta 2 in the hippocampus of patients with Alzheimer's disease neuropathology. *Neuroscience* **120**, 695-704.
- [53] Levenga J, Krishnamurthy P, Rajamohamedsait H, Wong H, Franke TF, Cain P, Sigurdsson EM, Hoeffler CA (2013) Tau pathology induces loss of GABAergic interneurons leading to altered synaptic plasticity and behavioral impairments. *Acta Neuropathol Commun* **1**, 34.
- [54] Najm R, Jones EA, Huang Y (2019) Apolipoprotein E4, inhibitory network dysfunction, and Alzheimer's disease. *Mol Neurodegener* **14**, 24.
- [55] Nyberg L, Andersson M, Lundquist A, Salami A, Wahlin A (2019) Frontal contribution to hippocampal hyperactivity during memory encoding in aging. *Front Mol Neurosci* **12**, 229.
- [56] Ramos B, Baglietto-Vargas D, del Rio JC, Moreno-Gonzalez I, Santa-Maria C, Jimenez S, Caballero C, Lopez-Tellez JF, Khan ZU, Ruano D, Gutierrez A, Vitorica J (2006) Early neuropathology of somatostatin/NPY GABAergic cells in the hippocampus of a PS1xAPP transgenic model of Alzheimer's disease. *Neurobiol Aging* **27**, 1658-1672.
- [57] Jimenez-Balado J, Eich TS (2021) GABAergic dysfunction, neural network hyperactivity and memory impairments in human aging and Alzheimer's disease. *Semin Cell Dev Biol* **116**, 146-159.
- [58] DiFrancesco JC, Tremolizzo L, Polonia V, Giussani G, Bianchi E, Franchi C, Nobili A, Appollonio I, Beghi E, Ferrarese C (2017) Adult-onset epilepsy in presymptomatic Alzheimer's disease: A retrospective study. *J Alzheimers Dis* **60**, 1267-1274.

- [59] Lyseng-Williamson KA (2011) Levetiracetam: A review of its use in epilepsy. *Drugs* **71**, 489-514.
- [60] Sanchez PE, Zhu L, Verret L, Vossel KA, Orr AG, Cirrito JR, Devidze N, Ho K, Yu GQ, Palop JJ, Mucke L (2012) Levetiracetam suppresses neuronal network dysfunction and reverses synaptic and cognitive deficits in an Alzheimer's disease model. *Proc Natl Acad Sci U S A* **109**, E2895-2903.
- [61] Shi JQ, Wang BR, Tian YY, Xu J, Gao L, Zhao SL, Jiang T, Xie HG, Zhang YD (2013) Antiepileptics topiramate and levetiracetam alleviate behavioral deficits and reduce neuropathology in APP<sup>swe</sup>/PS1<sup>dE9</sup> transgenic mice. *CNS Neurosci Ther* **19**, 871-881.
- [62] Cumbo E, Lorigi LD (2010) Levetiracetam, lamotrigine, and phenobarbital in patients with epileptic seizures and Alzheimer's disease. *Epilepsy Behav* **17**, 461-466.
- [63] Bakker A, Albert MS, Krauss G, Speck CL, Gallagher M (2015) Response of the medial temporal lobe network in amnesic mild cognitive impairment to therapeutic intervention assessed by fMRI and memory task performance. *Neuroimage Clin* **7**, 688-698.
- [64] Bakker A, Krauss GL, Albert MS, Speck CL, Jones LR, Stark CE, Yassa MA, Bassett SS, Shelton AL, Gallagher M (2012) Reduction of hippocampal hyperactivity improves cognition in amnesic mild cognitive impairment. *Neuron* **74**, 467-474.
- [65] Tolar M, Hey J, Power A, Abushakra S (2021) Neurotoxic soluble amyloid oligomers drive Alzheimer's pathogenesis and represent a clinically validated target for slowing disease progression. *Int J Mol Sci* **22**, 6355.
- [66] van Dyck CH, Swanson CJ, Aisen P, Bateman RJ, Chen C, Gee M, Kanekiyo M, Li D, Reyderman L, Cohen S, Froelich L, Katayama S, Sabbagh M, Vellas B, Watson D, Dhadda S, Irizarry M, Kramer LD, Iwatsubo T (2023) Lecanemab in early Alzheimer's disease. *N Engl J Med* **388**, 9-21.